Supplementary Information (SI) for Sensors & Diagnostics.
This journal is © The Royal Society of Chemistry 2026

A DSE–ESIPT-Active Organic Luminogen for "Off–On" Enantioselective Recognition of Chiral Amino Alcohols and Selective Hydrazine Sensing

Aakash Venkatesan, [a] Baru Venkata Naga Sahithi, [b] Francis Joy, [a] Rupali Nainesh Patel, [c] Aatika Nizam, [a*] Vasantha Veerappa Lakshmaiah [b*]

[a] Department of Chemistry, Christ University, Bangalore-560029, India

[b] Department of Life Sciences, Christ University, Bangalore-560029, India

[c] Department of Physics and Electronics, Christ University, Bangalore-560029, India

Corresponding author
Email ID: aatika.nizam@christuniversity.in
Email ID: vasantha.vl@christuniversity.in

2. Experimental procedure

2.1 Quantum Yield Calculation

The following equation was used to compute the quantum yield of the probe (ANMB) in various solvents, where x and sd are analogous to the sample and reference (quinine sulphate), respectively [1]. Quinine sulphate was found to have a 54% quantum yield in 0.5M H_2SO_4. Q, A, and I correspond to quantum yield, absorbance, and emission intensity (λ_{exc} = 370 nm).

$$Q_x = Q_{sd} \times \frac{A_{sd}}{A_x} \times \frac{I_x}{I_{sd}} \times \frac{\eta_x^2}{\eta_{sd}^2}$$

2.2 Preparation of stock solutions

The stock solution for the ANMB sensor was freshly prepared (c = 1.5 × 10^{-3} M) by dissolving the compound in DMF-Tris buffer (9/1, v/v, pH 7.4). Furthermore, solutions containing competitive analytes such as Cu^{2+}, Hg^{2+}, Co^{2+}, Al^{3+}, Cd^{2+}, Zn^{2+}, Ni^{2+}, Fe^{3+}, and Mg^{2+} were prepared to a concentration of 2 × 10^{-4} M, and biological analytes like Hydrazine were prepared to 12 mM. Thus, these solutions were used to formulate optical spectral changes using UV-vis and fluorescence spectroscopy.

2.3. Imaging of Hydrazine in Sprouts

Fresh chickpea seeds will be purchased from the local food market from Salem, Tamil Nadu. These chickpea seeds will be sprouted, utilising paper towel method and will be maintained on the cell plate. The sprouts will be incubated with 10 mM **ANMB** solution for 2 hr. Further,

they will be incubated with 20 µM hydrazine for 1 hr. The imaging of hydrazine will be observed by change in the photophysical property under UV light (365 nm) [2].

3. Results and discussion

3.1. Synthesis of ANMB

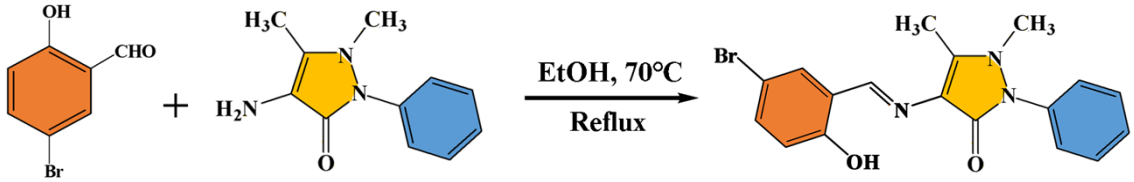

Scheme 1: Synthesis of ANMB

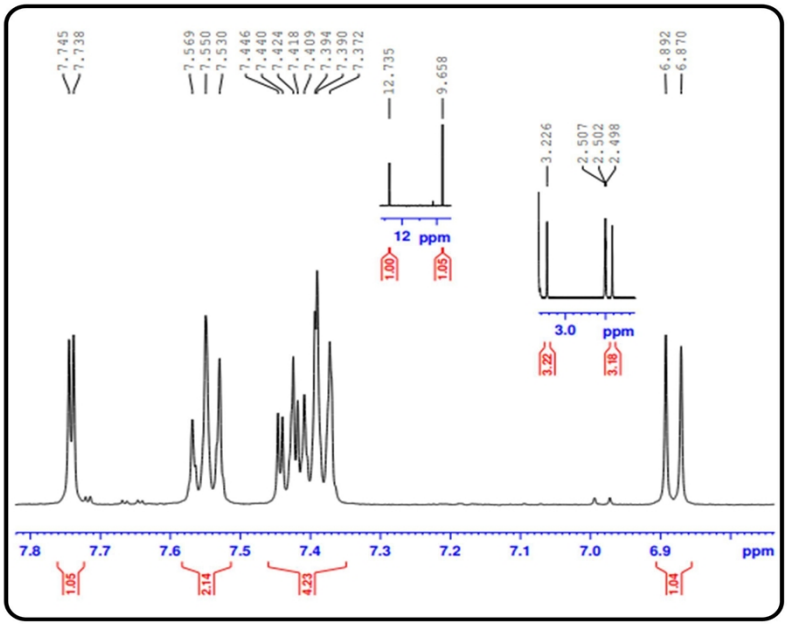

Figure S1: ^{1}H NMR spectrum of ANMB

3.2. Investigation of optical properties of ANMB

3.2.3. Solvochromic Characteristics of ANMB

Table S1: Photophysical data of ANMB in varying Solvents

Solvent	*λ_{max} (Emission)*	*λ_{max} (Excitation)*	*Quantum Yield*
DMSO	515	363	0.0136
DMF	510	364	0.0141

EA	520	361	0.0062
THF	519	362	0.0075
ACN	526	360	0.0111
$CHCl_3$	436, 522	359	0.0127
EtOH	428, 503	357	0.0109
MeOH	433	356	0.0024

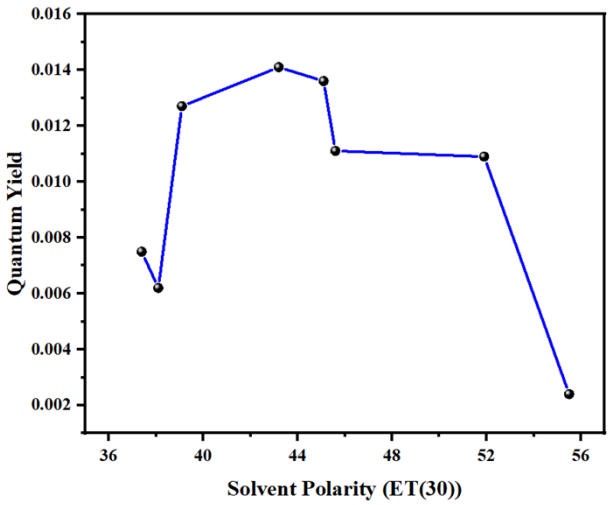

Figure S2: Photophysical data of ANMB in varying Solvents polarity

3.2.5. Aggregation Caused Quenching Characteristics of ANMB

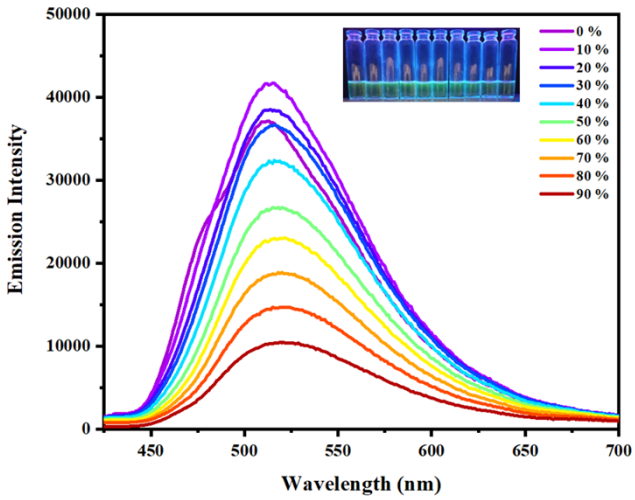

Figure S3: Emission spectra of ANMB on varying water fraction

3.2.6. Metal-Chelation Caused Quenching Characteristics of ANMB

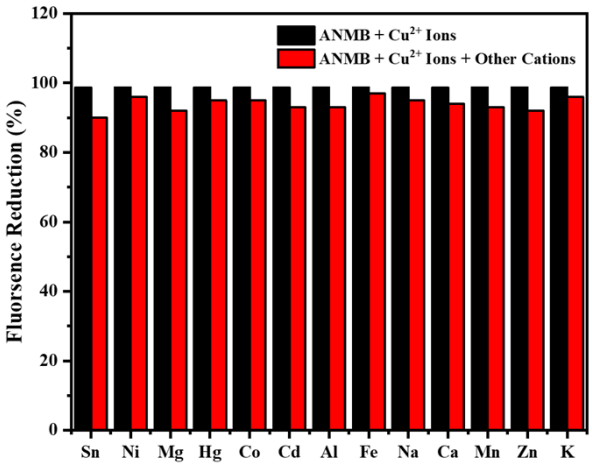

Figure S4: Interference studies for ANMB + Cu^{2+} system

3.2.6.3. Mathematical Model Studies

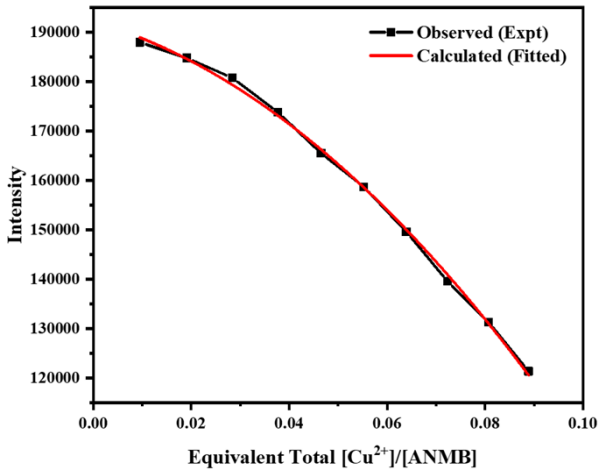

Figure S5: Bindfit plot for ANMB and Cu^{2+} system

3.3. Sensing of Biological Analytes and Biological Activity

3.3.1. Amino Alcohol response towards ANMB

3.3.1.1. Photoluminescence Studies

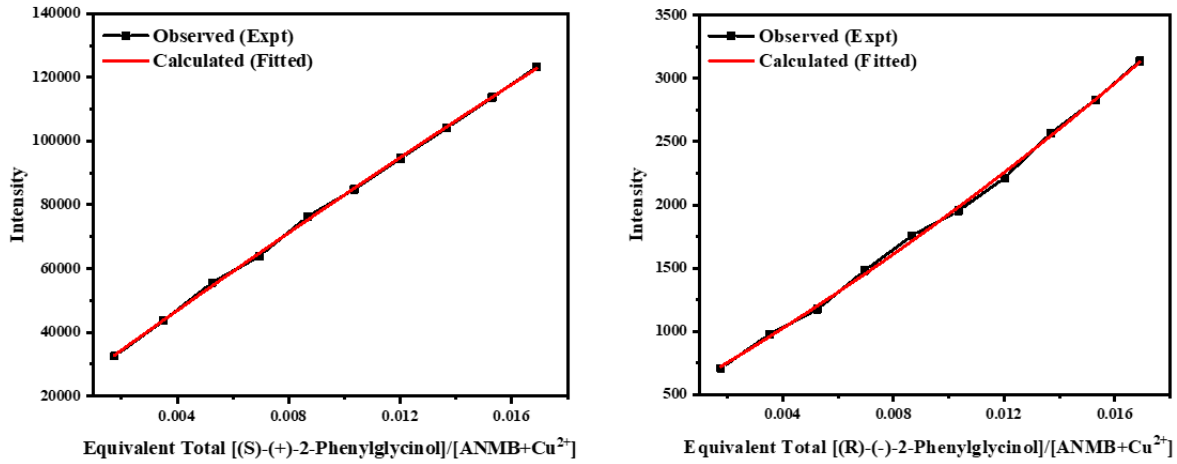

Figure S6: Bindfit plot for ANMB+Cu^{2+} and (a) (S)-(+)-2-Phenylglycinol (b) (R)-(-)-2-Phenylglycinol system

3.3.2. Hydrazine response towards ANMB

3.3.2.1. Photoluminescence studies

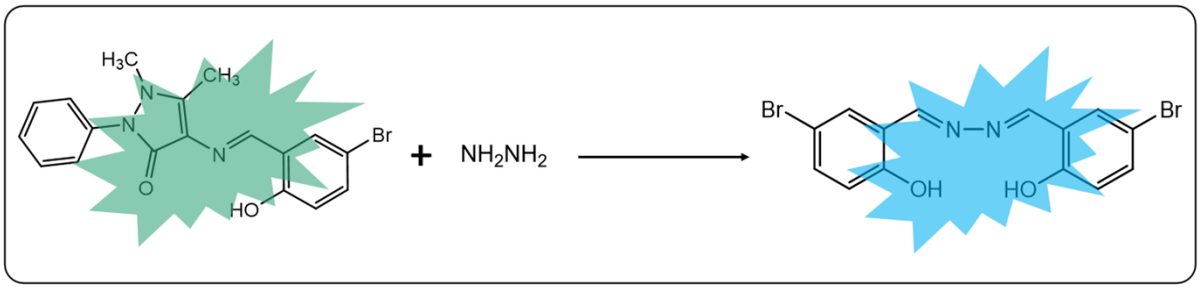

Scheme 2: Interaction of ANMB with Hydrazine

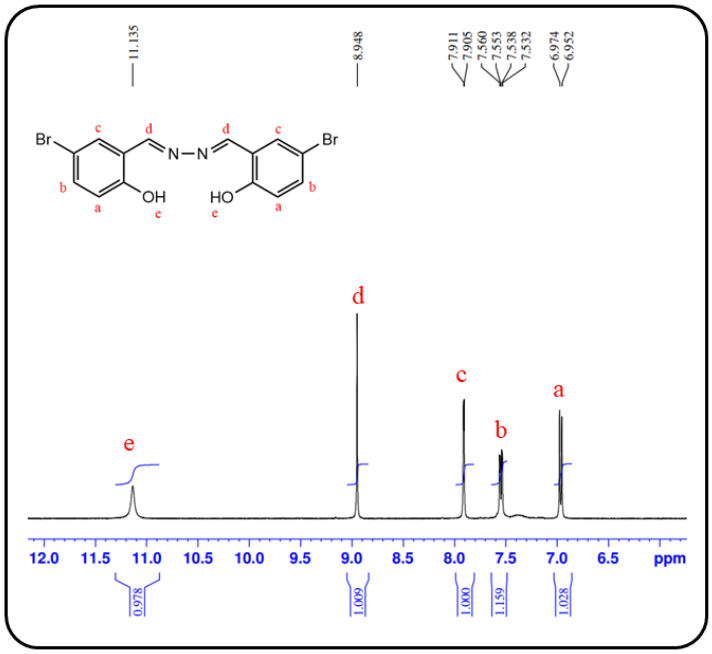

Figure S7: (a) ^{1}H NMR spectrum; (b) LC-MS spectrum of ANMB+NH_2NH_2

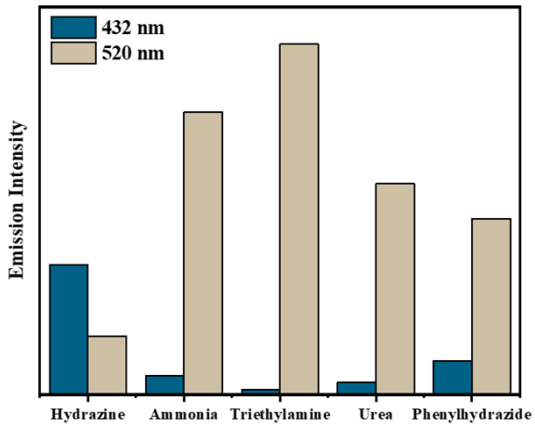

Figure S8: Selectivity studies for ANMB towards hydrazine

3.3.3. Molecular Docking Studies of ANMB

Table S2: Molecular interactions with amino acids of proteins (PDB ID: 4EJ4, 4U14, 5C1M)

S.No	*Proteins*	*Hydrophilic Interactions*		*Hydrophobic Contacts*		*No of H-Bonds*	*No of Total Bonds*	*Affinity kcal mol^{-1}*
		Residue (H-Bond)	*Length*	*Residue (Bond Type)*	*Length*			
				ILE52 (Alkyl)	-			
				TYR109 (Alkyl)	-			
				VAL197 (Pi-Alkyl)	-			
		GLU112 (Salt Bridge)		TRP114 (van de Waals)	-			
1	4EJ4	LYS108 (Pi-Cation)	-	VAL196 (van de Waals)	-	0	14	-7.8
		GLU112 (Pi-Anion)		CYS198 (van de Waals)	-			
		HIS301 (Pi-Anion)		ALA49 (van de Waals)	-			
				THR113 (van de Waals)	-			

			ALA195(van de Waals)	-		
			SER45 (van de Waals)	-		
			LEU225 (Alkyl)	-		
			PRO228 (Pi-Alkyl)	-		
			TRP525 (Pi-Pi Stacked)	-		
			ASN526 (van de Waals)	-		
			PHE124 (van de Waals)	-		
		LEU225 (H-Bond)	TYR529 (van de Waals)	-		
2	4EJU	TRP525 (Pi-Cation)	TYR506 (van de Waals)	-	1	15	-8.1
			TYR148 (van de Waals)	-		
			THR231 (van de Waals)	-		
			GLU227 (van de Waals)	-		
			SER226 (van de Waals)	-		
			ASP517 (van de Waals)	-		
			ASN513 (van de Waals)	-		
			PHE221 (Alkyl)	-		
			LEU232 (Pi-Alkyl)	-		
			MET205 (Pi-Sulfur)	-		
		THR220 (H-Bond)	LEU231 (van de Waals)	-		
3	5C1M	SER222 (H-Bond)	TRP228 (van de Waals)	-	3	11	-7.1
		SER222 (H-Bond)	PHE221 (van de Waals)	-		
			PRO201 (van de Waals)	-		
			PHE204 (van de Waals)	-		

3.3.4. ADME prediction results

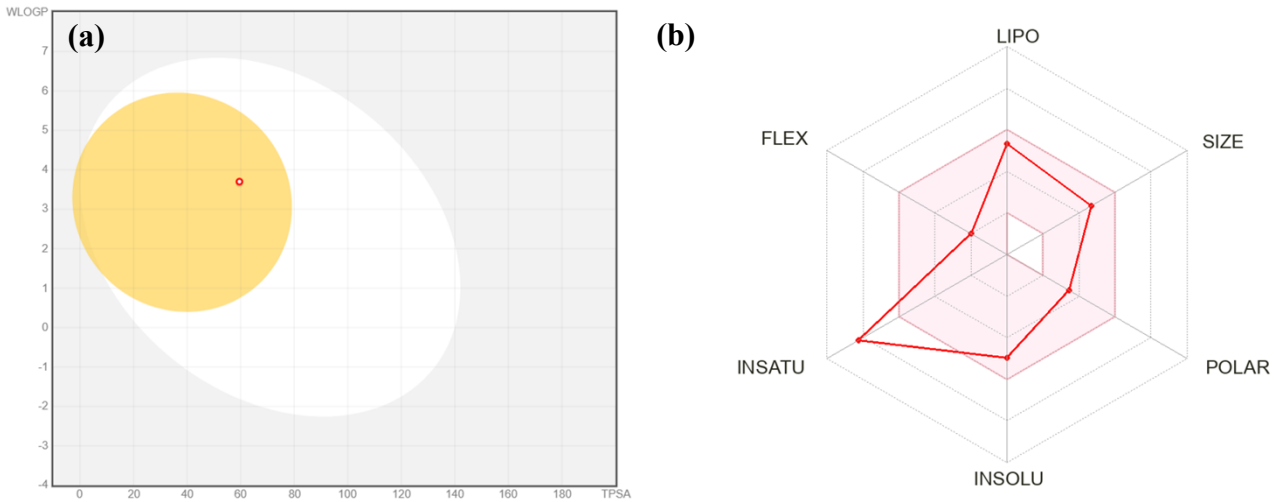

Figure S9: (a) Boiled egg diagram, (b) Bio-radar of ANMB for Oral Bio-availability

Table S3: ADME properties of ANMB

Physicochemical Properties

Formula	$C_{18}H_{16}BrN_3O_2$
Molecular weight	386.24 g/mol
Num. heavy atoms	24
Num. arom. heavy atoms	17
Fraction Csp3	0.11
Num. rotatable bonds	3
Num. H-bond acceptors	3
Num. H-bond donors	1
Molar Refractivity	99.68
TPSA	59.52 Å²
Lipophilicity	
Log $P_{o/w}$ (iLOGP)	3.13
Log $P_{o/w}$ (XLOGP3)	3.83
Log $P_{o/w}$ (WLOGP)	3.70
Log $P_{o/w}$ (MLOGP)	3.15
Log $P_{o/w}$ (SILICOS-IT)	3.65
Consensus Log $P_{o/w}$	3.49
Water Solubility	
Log *S* (ESOL)	-4.97
Solubility	4.10e-03 mg/ml ; 1.06e-05 mol/l
Class	Moderately soluble
Log *S* (Ali)	-4.78
Solubility	6.48e-03 mg/ml ; 1.68e-05 mol/l
Class	Moderately soluble
Log *S* (SILICOS-IT)	-5.60
Solubility	9.61e-04 mg/ml ; 2.49e-06 mol/l
Class	Moderately soluble
Pharmacokinetics	
GI absorption	High
BBB permeant	Yes
P-gp substrate	No
CYP1A2 inhibitor	Yes

CYP2C19 inhibitor	Yes
CYP2C9 inhibitor	Yes
CYP2D6 inhibitor	No
CYP3A4 inhibitor	No
Log K_p (skin permeation)	-5.94 cm/s
Druglikeness	
Lipinski	Yes; 0 violation
Ghose	Yes
Veber	Yes
Egan	Yes
Muegge	Yes
Bioavailability Score	0.55
Medicinal Chemistry	
PAINS	0 alert
Brenk	1 alert: imine_1
Leadlikeness	No; 2 violations: MW>350, XLOGP3>3.5
Synthetic accessibility	3.12

3.4. Real-time applications

3.4.3. Molecular logistic gate

The fluorescence recovery behaviour of ANMB in the presence of Cu^{2+} ions and amino alcohol as inputs, with emission peak at 512 nm as output, revealed an IMPLICATION logistic gate (**Figure S10a** and **S10b**). Additionally, Cu^{2+} ions and hydrazine as inputs with emission peaks at 512 nm and 432 nm as outputs exhibited a two-input INHIBIT logistic gate (**Figure S10c** and **S10d**).

(a)

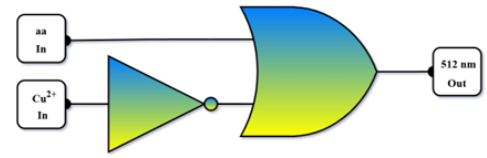

(b)

Input$_1$ (Cu^{2+})	*Input$_2$ (aa)*	*Output (λ_{max} 512 nm)*
0	0	1
1	0	0
0	1	1
1	1	1

Molecular logistic gate - IMPLICATION

(c)

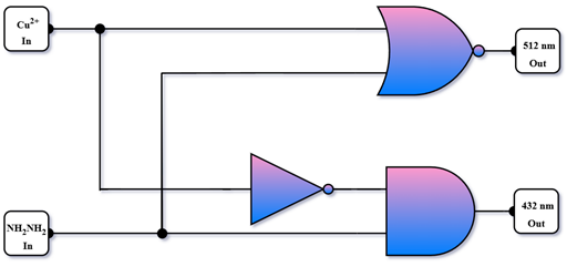

(d)

Input$_1$ (Cu^{2+})	*Input$_2$ (NH_2NH_2)*	*Output$_1$ (λ_{max} 512 nm)*	*Output$_2$ (λ_{max} 432 nm)*
0	0	1	0
1	0	0	0
0	1	0	1
1	1	0	0

Molecular logistic gate - Two-input INHIBIT

Figure S10: (a) Logistic diagram (b) The true table for the IMPLICATION gate (c) Logistic diagram (d) The true table for the two-input INHIBIT gate

3.4.4. Latent fingerprinting

Superior contrast in imaging LFPs requires a luminogen with a large Stokes shift and high brightness. **ANMB** has demonstrated its importance in LFPs because of its significant Stokes shift and longer emission wavelength. Thus, solid-state **ANMB** was used for LFP imaging. Hand cleansing is required prior to fingerprint collecting, and fingers must be lightly rubbed on the forehead or nose before being pressed into the substrate. The glass substrate was used to demonstrate the practical feasibility of utilizing **ANMB** for LFPs in forensic studies. The fingerprints impregnated on the glass substrate were dusted with **ANMB** using a brush that, when exposed to UV light (365 nm), emitted a bright green fluorescence. Since **ANMB** is adhesive, it adheres to perspiration and sebum found in LFPs that have fluorescent ridges and non-fluorescent furrows for simple visual identification. The picture was captured using a regular smartphone. The picture also clearly captures and illustrates primary and secondary level information about LFPs, such as bifurcation, core, curvature, and arch (**Figure S11**). The aforementioned finding indicates that **ANMB** can be employed as a fingerprint recognition technique to help solve criminal cases.

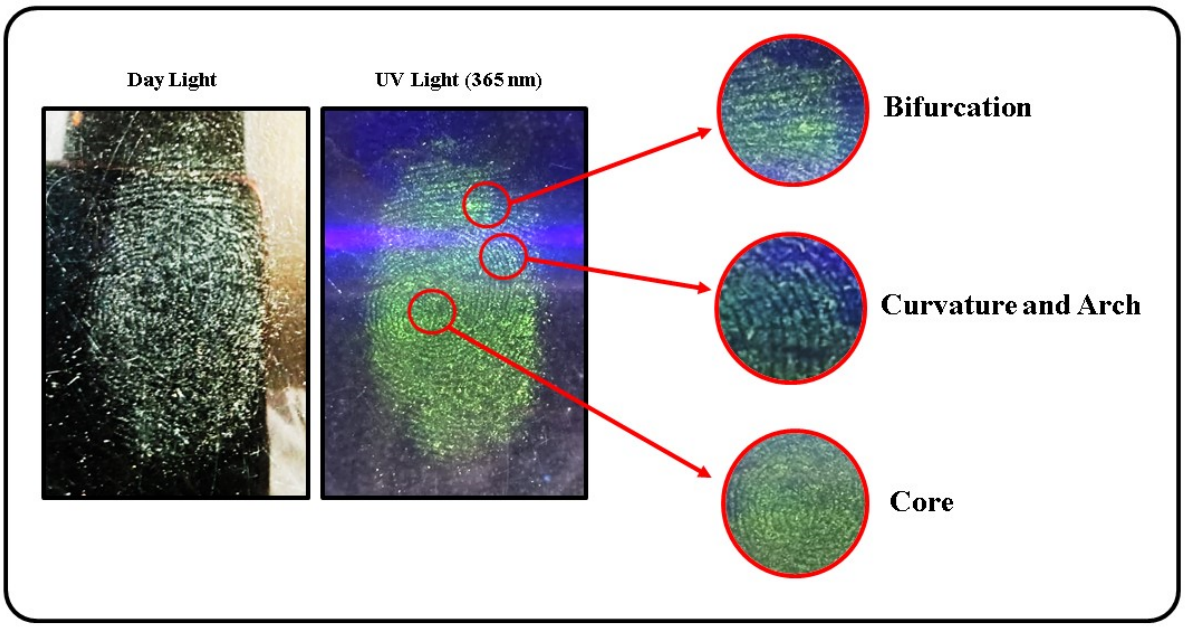

Figure S11: Photographic Images of LFPs by ANMB captured on a phone under UV irradiation and visible light showing primary and secondary level features

Reference

[1] Joy, F., V, A., Devasia, J., & Nizam, A. (2023). Excited-state intramolecular proton transfer ESIPT) salicylaldehyde Schiff bases: ratiometric sensing of ammonia and biologically relevant ions in solution and solid state. Supramolecular Chemistry, 34(11-12), 507-519.

[2] Chen, R., Li, B., Qin, X., Xing, S., Ren, H., Ma, F., ... & Niu, Q. (2024). A new carbazole based fluorescent probe with AIE characteristic for detecting and imaging hydrazine in living cells, mungbean sprouts, Arabidopsis thaliana, and practical samples. *Talanta*, *273*, 125953.